Dual Descriptor also reveals the Janus–Faced Behaviour of Diiodine

Jorge I. Martínez-Araya[*]

January 9, 2020

Abstract

The diiodine molecule as Janus–faced ligand was evidenced by Rogachev and Hoffmann [A.Y. Rogachev *et al., JACS*, 2013, **135**, 3262] through an exhaustive investigation based on the Molecular Orbital Theory (MOT), Natural Bond Orbital (NBO), and Energy Decomposition Analysis (EDA). In the present article the same conclusions were attained when applying the dual descriptor (DD or second–order Fukui function) on the same molecule. An advantage of DD lies on the fact of being an orbital–free descriptor, meaning that it is based only upon total electron density when written in its most accurate operational formula. In addition, the present work is an application of the generalized operational formula of the dual descriptor published in this journal in 2016 so allowing to predict the same coordination modes as experimentally known: bent "end–on" and linear "end–on"

Keywords: Dual descriptor, Second–order Fukui function, Janus–faced ligand, Bent "end–on" coordination mode, Linear "end–on" coordination mode. ■

[*]Departamento de Ciencias Químicas, Facultad de Ciencias Exactas, Universidad Andres Bello (UNAB), Av. República 498, Santiago, Chile.Tel: +56 2277 3957; E-mail: jorge.martinez@unab.cl

INTRODUCTION

Dual descriptor [or second order Fukui function] symbolized as $f^{(2)}(\mathbf{r})$ and proposed by Morell and coworkers[1,2], is an orbital–free local reactivity descriptor when is written in terms of total electron densities rather than frontier molecular orbital densities. Its main advantage lies in the fact that it provides more accurate information about local reactivities than the well–known Fukui functions. This is due to a kind of cancelation of relaxation terms when expressing the electronic density as an expansion of molecular orbital densities[3]. However, the presence of degeneracy in frontier molecular orbitals exerts an influence on local reactivity that, when ignored, leads to erroneous local reactivity information. Hence, an obvious question arises: how can we be accurate enough to yield 3D pictures of the dual descriptor based on its orbital–free operational formula and at the same time consider any possible degeneracy that could exist in frontier molecular orbitals?

The answer was published in this same journal through an accurate operational formula to be applied on closed–shell systems[4] to obtain 3D pictures of the dual descriptor. Said operational formula is based on total electronic densities while taking into account any possible degeneracy in frontier molecular orbitals as given by Eq.(1). Since it includes the degrees of degeneracy of HOMO and LUMO given by the integer numbers q and p, respectively, this operational formula is considered an improved version of the original one[1], thus making it more suitable to describe local reactivity:

$$f^{(2)}(\mathbf{r}) \;=\; \frac{\mathrm{q}\cdot\rho(\mathbf{r})^{\mathrm{p}+1}_{N+\mathrm{p}} - (\mathrm{p}+\mathrm{q})\cdot\rho(\mathbf{r})^{1}_{N} + \mathrm{p}\cdot\rho(\mathbf{r})^{\mathrm{q}+1}_{N-\mathrm{q}}}{\mathrm{p}\cdot\mathrm{q}}\,. \tag{1}$$

Superscripts ($\mathrm{p}+1$, 1, and $\mathrm{q}+1$) indicate the spin–multiplicity for each electron density and subscripts ($N+\mathrm{p}$, N, and $N-\mathrm{q}$) correspond to the total number of electrons associated to the respective electron density. The total number of electrons is represented by the letter N, meanwhile p and q stand for the degrees of degeneracy of the LUMO and HOMO respectively, which coincidently indicate the number of arriving electrons to the p–fold LUMO and leaving electrons from the q–fold HOMO.

Rogachev and Hoffmann[5] found that the diiodine molecule can react as an electron–acceptor or as an electron–donor depending on its counterpart. On the one hand, for instance, they discovered that the diiodine behaves as an electron–acceptor through a σ^*(I-I) orbital when interacting with the Pt atom of the $[(C_8H_{11}N_2)Pt(CH_3)]$, an organometallic compound. On the other hand, they also reported that diiodine behaves as an electron–donor towards the Rh_2–core of $[Rh_2(O_2CCF_3)_4]$, a metal–organic compound, through the σ^*(Rh-Rh) orbital. In the present work, the same conclusion concerning the double behavior of diiodine molecule is reached when using the operational formula given by Eq.(1); which has the advantage of not using molecular orbital theory due to its direct dependence upon total electronic densities.

METHODOLOGY

For this work, the software Gaussian16 was used[6]. From the Basis Set Exchange website (https://www.basissetexchange.org/), the def2–QZVPPD basis set[7], which includes diffuse functions for all atoms involved in the present work along with pseudo–potentials for the I, Pt, and Rh atoms, was selected and employed. Diffuse functions are mandatory to get a correct description of local reactivity given by the dual descriptor as demonstrated in a previous work[8]. Gusev suggested the use of the M06L functional[9] because it is accurate enough to compute thermodynamic parameters of chemical reactions involving organometallic and metal–organic complexes based on transition metals as the ones analyzed here.

It is important to clarify that for the Pt and Rh complexes, coordinates for the optimized geometry were obtained from the data published by Rogachev and Hoffman. Geometry optimizations were done solely on the diiodine molecule. Nevertheless, single point calculations were done on all optimized geometries. The route section for the optimization jobs was set to: M06L/GenECP SCF=(Tight,Fermi,MaxCyc=200,NoVarAcc,XQC) 5D NoSymm Int =(Grid=Ultrafine,acc2e=12) Guess=Huckel Opt=(VeryTight,CalcAll,MaxCyc=300). Single point calculations were done with the same level of theory, basis set, and SCF, Int, and Guess options. No symmetry restriction was set by means of the NoSymm command for all single point calculations and pure d functions were added to the diiodine molecule by means

of the option 5D.

The commands specified for the SCF either speed–up or guarantee convergence of the SCF cycles. Firstly, tight sets the energy convergence criterion to 10^{-8} Hartree. The option Fermi speeds up the convergence of the SCF cycles by broadening the gap between virtual and occupied orbitals by means of fractionally occupied orbitals around the Fermi energy during the SCF cycles[10]. The maximum number of SCF cycles was set to 200 to assure the convergence criterion is met and NoVarAcc maintains a high accuracy in the calculations from the very beginning of calculations, as opposed to the default option which is that the accuracy of the calculations increases with each step. Finally, XQC allows for a quadratic convergence of the SCF[11]; therefore speeding–up the process. The initial parameters (guess) for the SCF calculations were obtained with the Huckel method, which was indicated to Gaussian with Guess=Huckel.

For the integration process, setting the grid parameter to ultrafine[12] means that, using a minimal number of points, integration grids achieve a level of accuracy of 99 radial shells and 590 points per shell[13]. In addition, imposing acc2e=12 sets two–electron integral accuracy parameter to 10^{-12} Hartree. On the other hand, the convergence accuracy for the geometrical optimization calculations was set at 0.000002 for maximum force, 0.000001 for RMS (root mean square), 0.000006 for maximum displacement, and 0.000004 for RMS displacement with the VeryTight command. The CalcAll option in the Opt parenthesis computes the force constant at every point and with MaxCyc the maximum number of geometrical optimization steps was set to 300.

In order to work with Eq.(1), electronic densities must be obtained from the single point calculations. This was achieved using the cubegen subroutine, which constructed 3D pictures of the dual descriptor to yield the electronic densities. The arithmetic operations between these densities were carried out using the cubman subroutine. Both subroutines are included in the Gaussian 16 software package[6].

The values for the different parameters of Eq.(1) were set in accordance with the chemical nature of each species. For example, for the diiodine molecules $N = 106$ (the total number of electrons), p = 1 and q = 2. The values of p and q follow Hund's maximum multiplicity rule and take into consideration, respectively, the doubly degenerate HOMO and non–degenerate LUMO of the diiodine molecule (Table 2). Spin multiplicities are therefore set to 2 (coming from p + 1) and 3 (coming from q + 1). Eq.(1) then turns into Eq.(2):

$$f^{(2)}(\mathbf{r}) \;=\; \frac{2\cdot\rho(\mathbf{r})^{2}_{107} - 3\cdot\rho(\mathbf{r})^{1}_{106} + \rho(\mathbf{r})^{3}_{104}}{2}\,. \tag{2}$$

Because pseudopotentials included in the def2-QZVPPD basis set replace 28 electrons per iodine atom, the total number of electrons dealt with is 50 ($N = 106 - 2\cdot 28 = 50$), leading to the following definitive operational formula:

$$f^{(2)}(\mathbf{r}) \;=\; \frac{2\cdot\rho(\mathbf{r})^{2}_{51} - 3\cdot\rho(\mathbf{r})^{1}_{50} + \rho(\mathbf{r})^{3}_{48}}{2}\,. \tag{3}$$

Owing to the closeness among energies of molecular orbitals of transition metal complexes, an energetic threshold must be set by which to define degeneracy and hence the values for the variables p and q in Eq.(1) for the Rh and Pt complexes. It seems sensible to consider a degeneracy case when the energy difference between two neighboring molecular orbitals is equal or smaller than the 2 % of the HOMO–LUMO energy gap. Under this restriction the values for p and q have been set for both the Pt and the Rh complexes.

As a consequence, the same analysis performed on the diiodine molecule was done for each species, yielding three different expressions for Eq.(3) since 28 electrons are also replaced by a pseudopotential for each Rh atom in the $[Rh_2(O_2CCF_3)_4]$ complex ($N = 310 - 2\cdot 28 = 254$) and 60 electrons are replaced by a pseudopotential for the Pt atom in the $[(C_8H_{11}N_2)Pt(CH_3)]$ complex ($N = 160 - 60 = 100$), thus leading to the following operational formulae:

For the $[Rh_2(O_2CCF_3)_4]$ complex

$$f^{(2)}(\mathbf{r}) \;=\; \rho(\mathbf{r})^{2}_{255} - 2\cdot\rho(\mathbf{r})^{1}_{254} + \rho(\mathbf{r})^{2}_{253}\,. \tag{4}$$

For the $[(C_8H_{11}N_2)Pt(CH_3)]$ complex

$$f^{(2)}(\mathbf{r}) = \frac{2\cdot\rho(\mathbf{r})^{3}_{102} - 4\cdot\rho(\mathbf{r})^{1}_{100} + 2\cdot\rho(\mathbf{r})^{3}_{98}}{4}\,. \quad (5)$$

RESULTS

Diiodine molecule

When Eq.(3) is applied to the diiodine molecule in gas phase, after geometrical optimization at the M06-L/def2–QZVPPD level of theory, the interatomic distance is comparable to the experimental one (a 0.7 % of error with respect to the experimental iodine–iodine distance). Therefore, it can be stated that the level of theory employed reproduces the bond length within an acceptable accuracy as quoted by Table 1:

Geometrical Structure	**Theoretical**	**Experimental**
d(I–I)	2.6856	2.6663

Table 1: : Interatomic distances for the diiodine molecule given in angstroms.

Orbital	**Energy**
LUMO +2	0.01097
LUMO +1	0.00790
LUMO	-0.14633
HOMO	-0.22570
HOMO -1	-0.22570
HOMO -2	-0.28521

Table 2: Energies (in Hartrees) of molecular orbitals in the diiodine molecule.

A clear degeneracy of the HOMO and HOMO-1 orbital for the diiodine molecule, as shown in table 2, implies q = 2. On the other hand, there is no degeneracy regarding the

LUMO and thus p = 1.

Organometallic and metal–organic complexes

In accordance with the threshold criterion, a two–fold HOMO and two–fold LUMO appear in the $[(C_8H_{11}N_2)Pt(CH_3)]$ compound. The doubly degenerate frontier orbitals imply a value of 2 for both p and q. On the contrary, there is no degeneracy of the frontier molecular orbitals of $[Rh_2(O_2CCF_3)_4]$, in which case p and q equal 1. Energies of the nearest two virtual and two occupied molecular orbitals to the LUMO and HOMO, are quoted in Table 3 for $[(C_8H_{11}N_2)Pt(CH_3)]$ and Table 4 for $[Rh_2(O_2CCF_3)_4]$:

Orbital	**Energy**
LUMO +2	-0.00723
LUMO +1	-0.02063
LUMO	-0.02237
HOMO	-0.15881
HOMO -1	-0.16052
HOMO -2	-0.17734

Table 3: Energies (in Hartrees) of molecular orbitals in $[(C_8H_{11}N_2)Pt(CH_3)]$.

Orbital	**Energy**
LUMO +2	-0.12489
LUMO +1	-0.14026
LUMO	-0.18331
HOMO	-0.22617
HOMO -1	-0.22853
HOMO -2	-0.22863

Table 4: Energies (in Hartrees) of molecular orbitals in the $[Rh_2(O_2CCF_3)_4]$.

DISCUSSION

Different cuts of the dual descriptor are displayed for the diiodine molecule in Figure 1. According to the color code used here, Figure 2 indicates the electron flow coming in (green arrows) and going out (red arrows) from this molecule. Dark–colored lobes located at the upper and lower axial positions represent the electrophilic regions, while white–colored lobes surrounding iodine atoms are the nucleophilic regions. Notice that red arrows should be drawn all around both iodine atoms on planes perpendicular to the chemical bond, as if forming a disk around each iodine atom. However, for the sake of clarity only two red arrows per each imaginary plane have been drawn.

Figure 3 shows that the favorable interaction occurs through the Pt atom in such a way that this atom donates electrons towards one of the two atoms of diiodine. As observed, the most significative white–colored lobe of the Pt–based complex is located on the Pt atom, making it the most susceptible to undergo an electrophilic attack from the diiodine molecule through its electrophilic axial region represented by dark–colored lobes. Clearly the Pt–based complex reacts as a nucleophilic species and the diiodine molecule approaches perpendicularly on the plane of this Pt–based complex, so leading to the linear "end–on" coordination mode.

The opposite situation is depicted by Figure 4. In this case, the most reactive regions on the Rh–based complex are located around both metal atoms. According to the dual descriptor, these atoms are susceptible to undergo nucleophilic attacks and since the diiodine molecule is again the countpart molecule to react it uses its nucleophilic regions; represented by the white–colored lobes that equatorially surround the iodine atoms. Thanks to one of these nucleophilic lobes, the diiodine molecule approaches side by side towards the Rh–based complex so leading to the bent "end–on" coordination mode. Notice here that the diiodine molecule acts as a molecule that donates electrons towards the closest Rh atom of the metal complex which reacts as an electrophilic species.

CONCLUSIONS

Dual descriptor, an orbital–free local reactivity descriptor, reveals that the diiodine molecule exhibits a nucleophilic behavior through those directions that are perpendicular to the chemical bond, thus leading to the so–called bent "end–on" coordination mode. On the contrary, the same molecule shows an electrophilic behavior through axial directions (aligned to the iodine–iodine bond) which leads to the so–called linear "end–on" coordination mode. This example illustrates the capability of the dual descriptor to find the most reactive sites on a molecule leading to coordinations modes which are in agreement with experimental evidence thus complementing explanations grounded on theories like MOT, NBO, and EDA.

ACKNOWLEDGMENTS

The author acknowledges the financial support provided by FONDECYT grant N∘ 1181504 and also wishes to thank miss Alessandra Misad Saide for her valuable technical assistance to lead improving the writing of the article. In such a way, it also turned into a more pedagogical document for those colleagues and students interested in learning more about chemical reactivity from the perspective of the Conceptual Density Functional Theory and how to apply one of its reactivity descriptors.

References

1. Morell, C., Grand, A., Toro-Labbé, A., J. Phys. Chem. A, **2005**, 109, 205–212.

2. Morell, C., Grand, A., Toro-Labbé, A., Chem. Phys. Lett., **2006**, 425, 342–346.

3. Martínez-Araya, J.I., J. Math. Chem., **2015**, 53, 451–465.

4. Martínez-Araya, J.I., J. Comput. Chem., **2016**, 37, 2279–2303.

5. Rogachev, A.Y., Hoffmann, R., J. Am. Chem. Soc., **2013**, 135, 3262–3275.

6. Frisch, M.J., Trucks, G.W., Schlegel, H.B., Scuseria, G.E., Robb, M.A., Cheeseman, J.R., Scalmani, G., Barone, V., Petersson, G.A., Nakatsuji, H., Li, X., Caricato, M., Marenich, A.V., Bloino, J., Janesko, B.G., Gomperts, R., Mennucci, B., Hratchian, H.P., Ortiz, J.V., Izmaylov, A.F., Sonnenberg, J.L., Williams–Young, D., Ding, F., Lipparini, F., Egidi, F., Goings, J., Peng, B., Petrone, A., Henderson, T., Ranasinghe, D., Zakrzewski, V.G., Gao, J., Rega, N., Zheng, G., Liang, W., Hada, M., Ehara, M., Toyota, K., Fukuda, R., Hasegawa, J., Ishida, M., Nakajima, T., Honda, Y., Kitao, O., Nakai, H., Vreven, T., Throssell, K., Montgomery Jr., J. A., Peralta, J.E., Ogliaro, F., Bearpark, M.J., Heyd, J.J., Brothers, E.N., Kudin, K.N., Staroverov, V.N., Keith, T.A., Kobayashi, R., Normand, J., Raghavachari, K., Rendell, A.P., Burant, J.C., Iyengar, S.S., Tomasi, J., Cossi, M., Millam, J.M., Klene, M., Adamo, C., Cammi, R., Ochterski, J.W., Martin, R.L., Morokuma, K., Farkas, O., Foresman, J.B., Fox, D.J. *Gaussian 16 Revision B.01*, **2016**, Gaussian Inc. Wallingford CT.

7. Rappoport, D., Furche, F., J. Chem. Phys., **2010**, 133, 134105.

8. Martínez-Araya, J.I., Chem. Phys. Lett., **2019**, 724, 29–34.

9. Gusev, D.G., Organometallics, **2013**, 32, 4239–4243.

10. Rabuck, A.D., Scuseria, G.E., J. Chem. Phys., **1999**, 110, 695.

11. Bacskay, G.B,. Chem. Phys., **1981**, 61, 385–404.

12. Krack, M., Köster, A.M., J. Chem. Phys., **1998**, 108, 3226.

13. Lebedev, V., Skorokhodov, L., Russian Acad. Sci. Dokl. Math., **1992**, 45, 587–592.

Figure 1: Dual descriptor (DD) of diiodine at different isovalues given in atomic units. Purple spheres stand for iodine atoms, black–colored lobes represent positive values of DD ($f^{(2)}(\mathbf{r}) > 0$); white–colored lobes correspond to negative values of DD ($f^{(2)}(\mathbf{r}) < 0$).

Figure 2: On the left side, the iodine molecule; on the right side, dual descriptor of this molecule. Green arrows indicate the electron–acceptor (electrophilic) regions leading to a linear "end–on" coordination mode and red arrows show us the electron–donor (nucleophilic) regions thus leading to a bent "end–on" coordination mode.

Figure 3: On the left side, the $[(C_8H_{11}N_2)Pt(CH_3)]$ complex; on the right side, dual descriptor of this transition metal complex is displayed at an isovalue of 0.010 a.u. in order to highlight that the nearest region to the Pt atom is the most reactive to donate electrons; dual descriptor of diiodine is displayed at an isovalue of 0.0050 a.u. The resulting interaction between lobes of opposite colors leads to a linear "end–on" coordination mode.

Figure 4: On the left side, the $[Rh_2(O_2CCF_3)_4]$ complex; on the right side, dual descriptor of this transition metal complex is displayed at an isovalue of 0.010 a.u. so that Rh atoms are the most reactive to accept electrons; dual descriptor of diiodine is displayed at an isovalue of 0.0050 a.u. The resulting interaction between lobes of opposite colors leads to a bent "end–on" coordination mode.

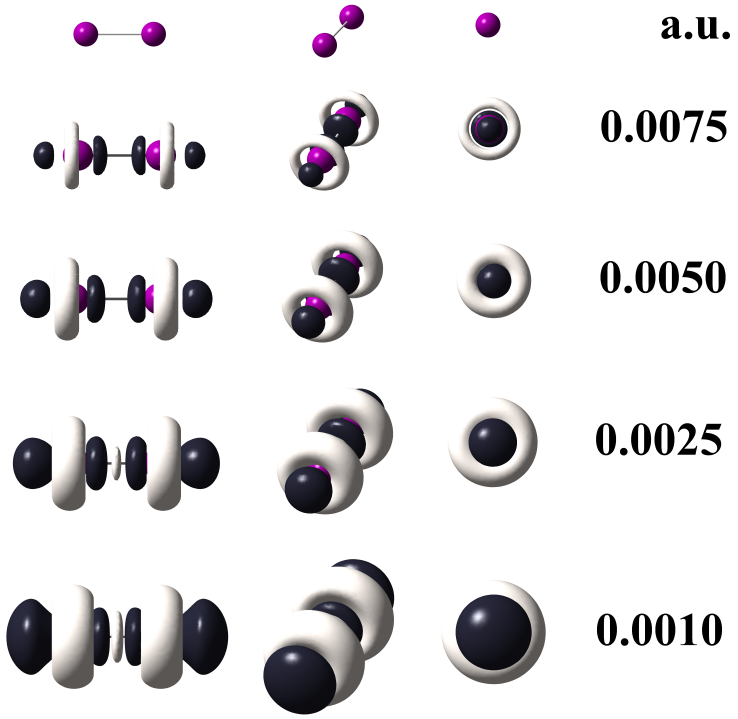

Figure 1
J. Martínez–Araya
J. Comput. Chem.

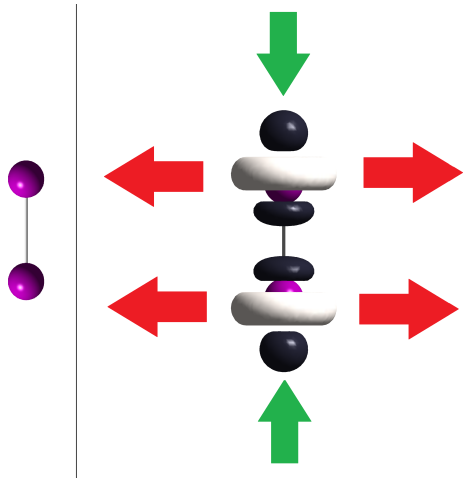

Figure 2
J. Martínez–Araya
J. Comput. Chem.

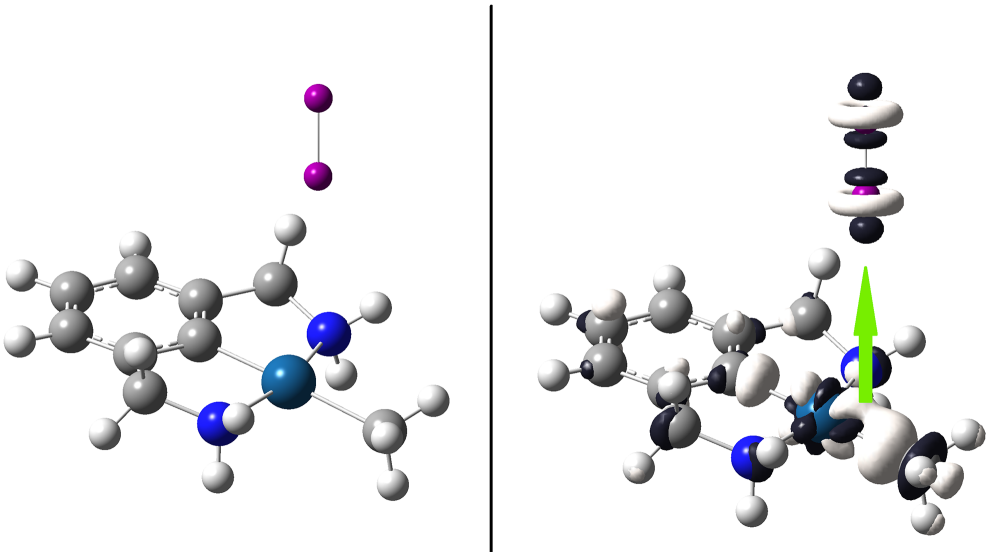

Figure 3
J. Martínez–Araya
J. Comput. Chem.

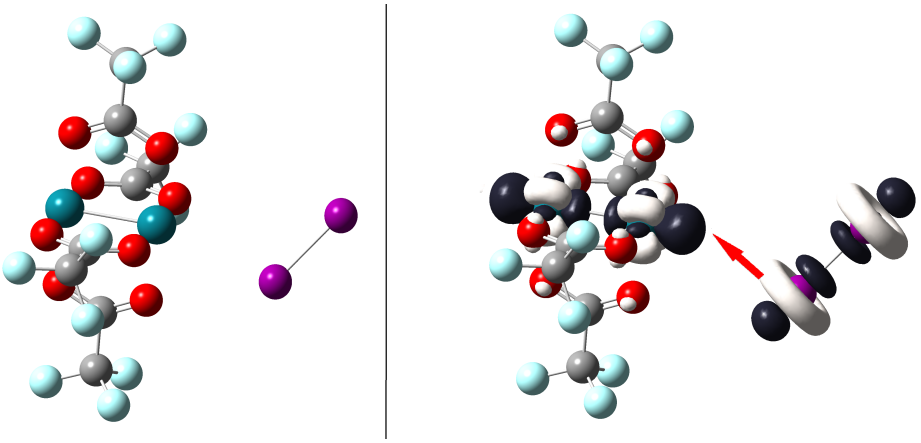

Figure 4
J. Martínez–Araya
J. Comput. Chem.